Recycling of Waste Tyre into Silica-Rubber Compounds for Green Tyre Application

Joyeeta Ghosh
MCKV Institute of Engineering
Sakrit Hait
Leibniz-Institut fur Polymerforschung eV
Soumyajit Ghorai
MCKV Institute of Engineering
Dipankar Mondal
University of Calcutta
Gert Heinrich
Leibniz-Institut fur Polymerforschung eV
Sven Wießner
Leibniz-Institut fur Polymerforschung eV
Amit Das
Leibniz-Institut fur Polymerforschung eV
Debapriya De (debapriyad2001@yahoo.com)
MCKV Institute of Engineering https://orcid.org/0000-0002-1500-2872

Research Article

Keywords: Devulcanization, Recycling of Tyres, Green Tyre Compounds, Reinforcement,

Posted Date: June 29th, 2021

DOI: https://doi.org/10.21203/rs.3.rs-460181/v2

Recycling of Waste Tyre into Silica-Rubber Compounds for Green Tyre Application

Joyeeta Ghosh[a], Sakrit Hait[b,c], Soumyajit Ghorai[a], Dipankar Mondal[d], Gert Heinrich[b,e], Sven Wießner[b,c], Amit Das[b,f*],Debapriya De[a*]

[a]Chemistry Department, MCKV Institute of Engineering, Liluah, Howrah 711204, India
[b]Leibniz-Institut für Polymerforschung Dresden e.V., D-01069 Dresden, Germany
[c]InstitutfürWerkstoffwissenschaft, Technische Universität Dresden, 01069 Dresden, Germany
[d]Department of Polymer Science & Technology, University of Calcutta, Kolkata 700009, India
[e]InstitutfürTextilmaschinen und Textile Hochleistungswerkstofftechnik, Technische Universität Dresden, 01069 Dresden, Germany
[f]Engineering and Natural Sciences, Tampere University, 33720 Tampere, Finland

Abstract

The prevention of detrimental effects to environment, owing to generation of a huge amount of rubber wastes, is a big challenge across the globe that warrants a thorough investigation of recycling and reuses waste of rubber products. In this spirit a sustainable development of a devulcanization process along with the production of value added devulcanized rubber is a task of hours. The present work describes a simultaneous devulcanization and chemical functionalisation process of waste solution styrene butadiene rubber (S-SBR). This kind of rubber is generally used as the main polymer component in silica filled tread rubber compounds for high-performance passenger car tyres. As-grown ethoxy groups on the functionalized devulcanized styrene butadiene rubber (D-SBR) are exploited for the coupling between silica and the devulcanized rubber chains. We compare the mechanical and dynamic mechanical performance of D-SBR with that of virgin SBR control composites. Covalently bonding interfaces developed from the pendent ethoxy groups of D-SBR and silanol groups on the silica surface offer a competitive and promising performance of the D-SBR based composites. We conclude that the present approach can be further utilized for the large-scale production of different rubber products with satisfied elastomeric performance.

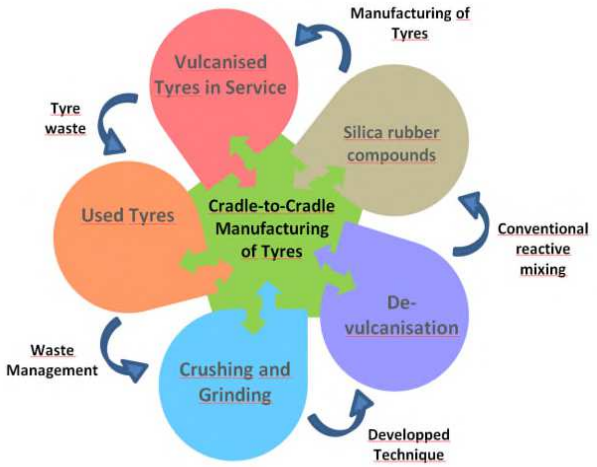

Keywords: Devulcanization, Recycling of Tyres, Green Tyre Compounds, Reinforcement,

*Corresponding author: e-mail: d.de@mckvie.edu.in (D. De); das@ipfdd.de (A. Das)

Statement of Novelty

A unique, cost effective and eco-friendly devulcanizing agent, tetrasulfide silane is used for devulcanization of scrap styrene butadiene rubber (SBR). The devulcanizing agent also facilitates the chemical functionalisation of devulcanized rubber and the so-grown functional groups are exploited for silica-rubber interfacial interaction. The addition of devulcanized SBR (D-SBR) into fresh SBR improves tensile strength, tear strength, elongation at break and abrasion resistance of the composite due to strong interfacial adhesion among fresh rubber, devulcanized rubber and silica. The present research elucidates the production of devulcanized rubber compounds for green tyre (energy efficient tyre) application. Furthermore, the higher tensile strength of the composite makes its importance for the use of devulcanized rubber in different product applications. The curing and processing parameters were also found not to be alerted which is much desired for the production of rubber component like tyres. This research is an initiative to prepare value added devulcanized rubber with superior product performance for attracting the rubber industry.

Introduction

The development of an efficient devulcanization process of discharged crosslinked rubber products, for example, tyres and other various auto parts, is a challenging task in this 21st century. The worldwide tyre production and waste generation scenario indicates that about 1.7 billion new tyres are produced in a year and over 1 billion waste tyres are spouted to the environment per year [1]. Due to three-dimensional covalently crosslinked network structure and the presence of many chemical additives, vulcanized rubber is not degradable by natural biological processes or by other chemical means like hydroxylation, oxidation etc. As a result, waste rubber creates serious environmental hazards [2]. So far, a number of different methods are introduced like mechanical [3-6], mechanochemical [7-12], microwave [13-15] and ultrasound [16,17] treatments. However, the desired level of devulcanization to regenerate the raw rubber has not been attained. It is worth mentioning that a straight complete recirculation of devulcanized rubber compounds into high-performance rubber products is not realized so far because of the poor mechanical performance of the devulcanized rubber products. However, a partial replacement of fresh rubber by devulcanized rubber is reported as possible and leads to adequate properties of the final rubber product [18, 19].

A specific treatment route describes the mechano-chemical devulcanization of ground tyre rubber in presence of bitumen and three different types of additives such as peptizer (P300), organic peroxide [di(2-tert-butyl-peroxyisopropyl) benzene] and vulcanization accelerator (tetramethylthiuramdisulphide, TMTD) [20]. In this case the vulcanized rubber can be reclaimed to a reasonable degree. Detailed studies onthe extent of reclaiming clearly specify that the used additives have a significant influence on the rubber processing, as well on the physico-mechanical and thermal properties of the reclaimed ground tyre rubber (GTR). Furthermore, it

was shown that the GTR can be used as component in efficient rubber blends, e.g. in combination with fresh nitrile butadiene rubber (NBR). In another work, allow molecular weight disulfide based organic compound is used to devulcanize waste ethylene propylene diene monomer (EPDM) rubber which was then mixed with fresh EPDM in different proportions (20 – 40 wt%) [21]. The results indicated that optimum cure- and scorch-time of the rubber blend were not affected uptoan added amount of 40 wt% of reclaimed EPDM. However, mechanical properties like tensile strength and elongation at break of the revulcanized blends were improved up to 14% and 26%, respectively. Different proportions (20 wt % to 60 wt %) of mechano-chemically devulcanized GTR can be revulcanized in a composition with natural rubber (NR) and polybutadiene rubber (BR) in a 70:30 proportion [22]. Here, reclaiming of GTR can be carried out using TMTD in the presence of spindle oil, a paraffin-based rubber process oil. The evaluation of curing characteristics of NR-BR/devulcanized rubber (DR) vulcanizates indicates that the optimum cure time decreases with DR content, andthe observed improvement of mechanical properties of the vulcanizates is attributed to the enhanced interfacial interaction between DR and NR-BR matrix. A cost-effective rubber blend based on 92 phrfresh NBR and 8 phr devulcanized NR is prepared and, subsequently, an evaluation of the mechanical properties of the vulcanizate was performed by using highly reinforcing nanofiller. The nanofillers were synthesized by condensation reactions between terephthaloyl chloride (TPC) with bis(4-aminophenyl) sulfone (BAPS) and bisphenol polyesteramide sulfone (PEAS) [23]. The results indicatethat the addition of PEAS improves the compatibility between NBR and reclaimed NR and enhances the effective crosslink density of the vulcanizates through physical interlocking leading to an increase of the tensile strength and decrease of the elongation at break of the vulcanizates. However, the amide and ester groups of PEAS affect the thermal stability of the

vulcanizate up to 420ºCas compared to neat NBR. Devulcanized rubber prepared from GTR using the microwave method can be mixed with styrene butadiene rubber (SBR) to develop new rubber compounds for further revulcanization [24]. It is observed that the devulcanized rubber/SBR composites offered improved frictional properties on nonabrasive surfaces and a significant rise in mechanical properties as compared to that of the SBR/GTR composites. Thermoplastic vulcanizates (TPVs) are prepared by mixing mechano-chemically devulcanized GTR (DR)/polypropylene (PP)/EPDM to study the effect of peroxide curing and γ-radiation on mechanical, thermal and structural parameters of the developed composites [25]. Use of1 phrdicumyl peroxide (DCP) and 25 kGy γ-radiation dosecan offer promising mechanical properties of the composites. Thermo-mechanical devulcanization of GTR is carried out at different temperatures (60, 120 and 180ºC) using a co-rotating twin screw extruder and the reclaimed rubbersare mixed with fresh SBR in 10 to 50 wt% [26]. It is found that the SBR vulcanizates containing devulcanized rubber lead to higher glass transition temperatures as compared to the vulcanizates containing untreated GTR. Grinding of waste rubber in the mills with ultrasonic activation can lead to the formation of a crumb rubber with particle size distribution in the range of 100 to 150 μm which can be used in different rubber composition as a replacement of devulcanizedrubber [27]. The experimental results demonstrate that replacement of regenerated rubber by a large proportion crumb rubber can lead to significant enhancement of tensile strength and elongation at break of the vulcanizates. Foaming of devulcanized ground tyre rubber (DGTR) as an alternative to natural rubber was developed and various applications such as cushioning, heat insulation, sound absorption etc. were discussed [28]. The effects of ethylene vinyl acetate (EVA), sodium carbonate as blowing agent and dicumyl peroxide (co-curatives) on the DGTR propertiesare studied and it is found that the

density and hardness of the foam decreased with increasing sodium bicarbonate content because of the formation of a higher number of voids by the released carbon dioxide gas. However, the density and hardness of the composites were found to be enhanced with increasing EVA content. Crosslinked rubber powder was mechano-chemically modified through 2,2/-dibenzothiazole disulfideat high shearing condition with the help of a twin-screw extruder at 100^{o}C [29]. In the study both unmodified rubber powder and chemically blended rubber powder were treated in the extruder to form mechanically modified and mechano-chemically modified rubber powder (MCRP), respectively. This chemical modification results a better processing characteristic and improved mechanical properties of MCRP/NR composites. A waste-to-product method was developed by hot-pressing technique to prepare membranes having gas permeance and separation characteristics using reclaimed tyre rubber as the polymer precursor [30]. The mechano-chemical devulcanization of waste rubber powder by bis[3-(triethoxysilyl)propyl]tetrasulfide was first developed by Ghorai et al. [8] but the efficacy of bis[3-(triethoxysilyl)propyl]tetrasulfide for physico-chemical reclaiming of GTR at two different operating temperatures, 170^{o}C and 190^{o}C was examined in [31]. They also reported that devulcanized GTR was very useful for the fabrication of a single electrode triboelectric nanogenerator (SETNG) which might produce electric energy during sliding friction. SETNG made of reclaimed rubber at 170^{o}C produced more output voltage than that of the reclaimed rubber at 190^{o}C, and exhibited distinct tactile sensation towards different objects such as human finger, latex rubber glove, cotton glove and polytetrafluroethtlene (PTFE) sheets.

In this work mechano-chemical devulcanization and simultaneous functionalization of commercially available waste SBR were done by using bis(3-triethoxysilyl propyl) tetrasulfide (TESPT) and subsequently the devulcanized rubber (D-SBR) is utilized to prepare new rubber

composites using silica as additional reinforcing agent. It is known that silica-based rubber composites are found to be most suitable for energy efficient so-called green tyre production, and in this work D-SBR is expected to have chemical groups that can allow to establish a direct chemical coupling between externally added silica with rubber chains. With the developed recycled silica-rubber composites, systematic characterizations of chemical modification of the D-SBR, the effect of D-SBR on the structure property relationship are thoroughly investigated. Likewise, underlying strong reinforcement mechanism by the chemical interaction of D-SBR (with grafted TESPT fragments) and silica are demonstrated that may pave the way to produce silica based recycled rubber composites for green tyre applications.

Experimental

Materials

30-40 Mesh SBR crumb rubber is procured from Maheswari Crumb Industries, India. The rubber hydrocarbon and carbon black content in SBR are 40-45wt% and 40wt% respectively. Devulcanized SBR (D-SBR) is prepared from SBR crumb through mechanochemical devulcanization by bis(3-triethoxysilyl propyl) tetrasulfide (TESPT), a dual function tetrasulfide devulcanizing agent as reported in the previous paper [9]. Styrene butadiene rubber (SBR-1502) (Synthetics and Chemicals Ltd., India), bis(3-triethoxysilyl propyl) tetrasulfide (TESPT) (Acros Organics, USA) as devulcanizing agent, zinc oxide (S.D. Fine Chem., India), stearic acid (LobaChemie, India), sulphur(S.D. Fine Chem., India), N-cyclohexyl-benzothiazyl-sulphenamide (CBS)as rubber ingredients and toluene (S.D. Fine Chem., India) as solvent were used without further purification. The precipitated silica (Ultrasil VN-3) with

specific surface area about 200 m^2/g was supplied by Evonik Resource Efficiency GmbH, Wesseling, Germany.

Preparation of devulcanized SBR (D-SBR)

100 g of SBR crumb is mixed with 6 mL of bis(3-triethoxysilyl propyl) tetrasulfide (devulcanizing agent) and 10 g of aromatic oil at room temperature and subsequently transferred to a two-roll mixing mill followed by mixing at a friction ratio of 1:1.25 for 40 min at ~70 to 80ºC.It is seen that with progress of milling a band formation occurs in the roll and the scrap powder material is transformed to homogeneous elastomeric material. The physical characteristics of D-SBR like sol content, crosslink density, and degree of devulcanization are found to be 25%, 0.306×10^{-3}mol/cm^3, 72.3% respectively. The Mooney viscosity ML(1+4) 100ºC was found to be 22.

Preparation of SBR/D-SBR/Silica composites

Virgin SBR, different proportions of D-SBR and compounding additives such as ZnO, stearic acid, sulphurand CBS were carried out for 10 min at room temperature on a two-roll mixing mill. Compound formulations are presented in Table 1. Formulation 1 contained no D-SBR and formulations 2-6 comprised with various proportions of D-SBR from 20-60 wt.%.A fixed amount of silica (30 phr) is incorporated into the SBR/D-SBR blend compounds. This mixing step is continued for 15 min at 80ºC in the same two-roll mill. Here in all the formulations the compounding ingredients such as ZnO, stearic acid, sulphur and CBS are added proportionally based on 100g rubber irrespective of the amount of D-SBR, as it was published by the authors [32] that the vulcanization additives accrued from parent compound are

inactive.SBR/D-SBR/SiO_2 composites prepared using different amount of D-SBR having 0, 20, 30, 40, 50 and 60 phr D-SBR are designated as D-0, D-20, D-30, D-40, D-50 and D-60 respectively.

Characterization of SBR/D-SBR/Silica composite

The curing behavior of SBR(control) and different SBR/D-SBR/Silica composites is studied with an Elastograph 67.12 (Göttfert, Germany) at 150ºC. The samples are then vulcanized in a compression molding machine at 150ºC and 35 MPa pressure for the respective optimum cure time ($t = t_{90}$) obtained from the rheographs.

In order to study the polymer-filler interaction as well as the crosslinking density of the composites, the tensile stress-strain data were used to the Mooney-Rivlin equation [33, 34]:

$$\frac{\sigma}{\lambda-\lambda^{-2}} = 2C_1 + \frac{2C_2}{\lambda} \quad (1)$$

where the term in the left-hand side is known as the reduced stress (σ_r) and the term C_1 and C_2 are the Mooney-Rivlin constants. The C_1 and C_2 values can be obtained by plotting of reduced stress versus reciprocal extension ratio ($^1/_\lambda$). The constant C_1 here related to an effective crosslink density [35]. Equation (1) can be used directly to an unfilled elastomer system. However, in the presence of hard incompressible filler particles, a correction can be done by consideration of strain amplification effect (x), using modified Bachelor and Green equation (Domurath et al, 2015)

$$x = 1 + 2.5\phi + 7.6\phi^2 \quad (2)$$

where ϕ is the volume fraction of silica. To avoid complexity the volume fraction of the filler from the original crumb rubber is not considered here. The extension ratio is represented by λ and is evaluated from $\lambda = 1 + \varepsilon x$, where ε is the strain.

A Mooney-Rivlin crosslink density (ν_{MR}) can be evaluated from the constant C_1 with the following equation [36]

$$\nu_{MR} = \frac{C_1}{RT} \quad (3)$$

where R and T are the universal gas constant and the measurement temperature in Kelvin scale, respectively.

In order to see the dispersion of silica in the composites, scanning electron microscopy (SEM) analysis of the samples was carried out by Zeiss EVO-MA10 at 0° tilt angle after coating the surface of the sample with sputtered gold. For this study the samples were broken in liquid nitrogen and the fractured surface of samples were examined. Fourier transform infrared spectrum (FTIR) of the composites was recorded in the ATR mode using Bruker, GmbH (Model: ALPHA), FTIR spectrophotometer. Tensile and tear strength of the composites were tested at room temperature (25°C)by Universal Tensile Machine (DigiUTM-2000V) as per ASTM D 412 and ASTM D 624 norms respectively.

The abrasion resistance of the composites was measured using DIN abrasion tester following ASTM D 5963.

To understand the amount of low molecular fragments and the thermal degradation behavior of SBR/D-SBR/silica composites thermogravimetry analysis (TGA) was carried out using a thermogravimetry analyzer (Model: Netzsch, Germany STA 449C) in nitrogen atmosphere at heating rate 10ºC/min. The analysis was carried from room temperature (25°C) to600 °C and the values presented were based on residual contents at 600 °C.

The calorimetric glass transition temperature (T_g) was measured using differential scanning calorimetry (DSC). Measurements were performed in the temperature range -100°C to 25 °C in

nitrogen atmosphere (purge) with a heating rate of 10 °C/min using DSC instrument (Model: Netzsch, Germany, Model No. 204 F1).

The dynamic mechanical properties like storage modulus ($E^{/}$), loss modulus ($E^{//}$) and loss tangent($\tan\delta$)of the composites were analyzed by an Eplexor 2000N (Gabo Qualimeter, Ahlden, Germany) at a frequency of 10 Hz in the tension mode with 1% static pre-strain and 0.5% oscillating dynamic strain. The tests were performed in the temperature range -100 to100 °C with a heating rate of 10°C/min under liquid nitrogen flow.

Table 1. Compound formulation and curing characteristics of SBR/D-SBR/silica blend system

	Sample Code					
	D-0	D-20	D-30	D-40	D-50	D-60
Materials (phr)						
SBR (SBR-1502)	100	80	70	60	50	40
DeVulcSBR	-	20	30	40	50	60
Curing characteristics						
t_{10}, min	16.54	5.43	4.92	4.75	2.26	4.39
Optimum cure time (t_{90}, min)	43.93	22.59	24.18	30.58	31.14	32.0
M_L (Nm)	0.21	0.21	0.25	0.22	0.14	0.41
M_H (Nm)	1.03	1.36	1.53	1.63	1.77	1.93
Extent of cure (M_H-M_L) (Nm)	0.82	1.15	1.28	1.41	1.63	1.52
Cure rate index (min^{-1})	3.65	5.83	5.19	3.87	4.67	3.62

Compound formulations: zinc oxide: 5 phr; stearic acid: 2 phr; sulphur: 1.8 phr and CBS: 1.2 phr and silica: 30 phr added in all the formulations. 'phr' stands for parts per hundred gm of rubber.

Results and Discussion

Curing characteristics

The cure behavior of the compounds is shown in Fig. 1.It is evident from this figure (Fig. 1a) that devulcanized rubber (without curatives) does not undergo any typical crosslinking reaction but at the very beginning the torque is suddenly raised and reaching 2 Nm torque value and after that a slight falloff of the respective value is noticed. After addition of sulphur curatives the compound offers a steady increment of the rheometric torque indicating a gradual progress of

thecrosslinking reaction of the matrix. The fact can be explained by the presence of active crosslinking sites in D-SBR [9] (Ghosh et al. 2018).

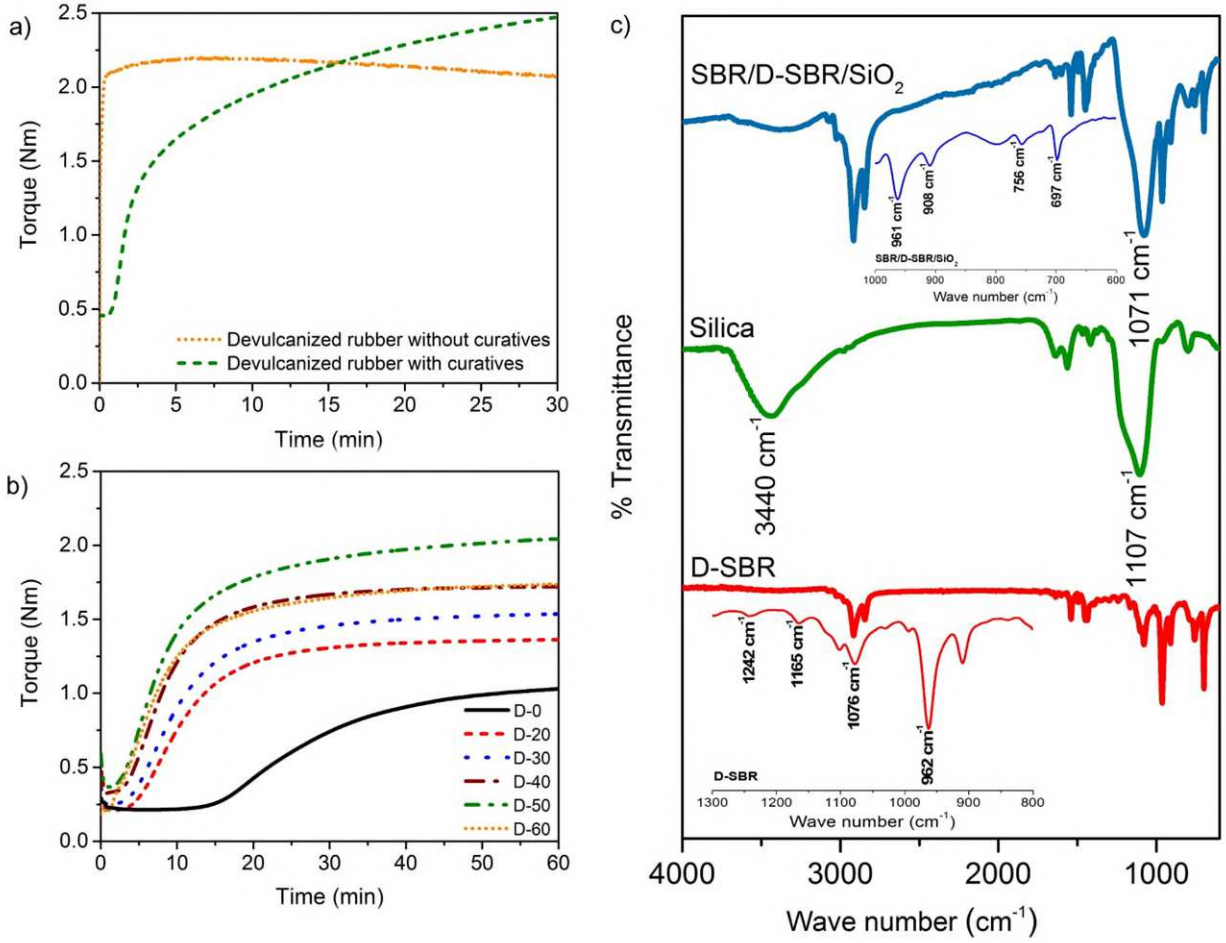

Figure 1: Curing behavior of a) only D-SBR in presence curatives and without curatives, b) SBR/D-SBR/Silica compound, c) FTIR of D-SBR, silica and SBR/D-SBR/silica

Most probably, owing to the high viscosity the 100% devulcanized compound without curatives shows such behavior (sudden increment of torque) but during the addition of curatives the rubber compound undergoes mastication and chain secession processes and resembles the behavior like a typical fresh rubber compound. From this study it is clear that regeneration of the double bond is taking place during devulcanization reaction and these double bonds are offering crosslinking reaction when the compounds are treated with sulphur based curatives. All the compounds with D-SBR show enhancement of curing torque as compared with pure SBR (fresh) (Fig. 1b). The

slow curing nature of pure SBR (D-0) is expected due to presence of silica. The silica absorbs the curatives resulting such marching and slow curing process. It should be mentioned here that silanization process is not done to this particular case. It is also seen from the figure that most of the compounds showed a plateau like curing behavior. The plateau nature of the compounds is maintained at 150 °C for 60 min which may indicate the superior aging characteristic of the respective cured samples. Thus, this kind of plateau type curing curve of all the compounds is preferred as it ensures the formation of stable crosslinking network [37, 38]. Since the cure properties varied with the concentration of D-SBR, therefore, scorch time (t_{10}), optimum cure time (t_{90}), minimum torque (M_L), maximum torque (M_L) and cure rate index are presented in Table 1. From this table it is evident that for all D-SBR containing samples display delayed optimum curing time (t_{90}). Simultaneously, t_{10} values gradually decrease with the increased of the devulcanized rubber content and the respective values are much lower than that of the control formulation (D-0) without any D-SBR portion. This indicates that accelerator compounds are not adsorbed on the silica surface due to chemical interaction between the pendent ethoxy of D-SBR and hydroxyl group of silica (Scheme 1). The increasing trend of optimum cure time with D-SBR loading is obvious because of mainly lack of sufficient active double bonds in the devulcanized rubber compounds as compared with fresh rubber. The increasing trend of rheometric torque with devulcanized rubber content is not only because of the presence of crosslinked gel and carbon black present in the devulcanized rubber but also for stronger interfacial interaction among silica, SBR and D-SBR. Finally, because of the interplay between curing activity of pure SBR and reinforcing activity of D-SBR the maximum development of torque is found to be highest with D-50 and with higher proportion of D-SBR the final value is further decreased.

FTIR analysis

Fig.1c shows the FTIR spectra of D-SBR, silica and SBR/D-SBR/Silica. As during devulcanization fragmented TESPT is attached to D-SBR [11], the characteristic absorption peaks of $Si-O$ cage like stretching mode at 1165 cm^{-1}, $Si-O$ stretching at 1078 and 965 $cm^{-1}$and symmetric $Si-C-H$ bending at 1242 cm^{-1} are noticed, pointing out the chemical attachment of fragmented TESPT in D-SBR. The FTIR spectra of silica shows the broad peak of $-OH$ stretching at 3446 cm^{-1} and $Si-O-Si$ stretching at 1105 cm^{-1}, whereas in SBR/D-SBR/Silica composite the peak of $-OH$ stretching does not appear. Nevertheless, the characteristic peak of $Si-O-Si$ stretching at 1070 cm^{-1} clearly indicates the rubber – filler interaction through the primary silanization reaction between the pendant ethoxy group of D-SBR and hydroxyl group on the silica surfaces through a direct condensation reaction or a secondary silanization reaction. In the last case the hydrolysis of the adjacent pendant ethoxy groups of the D-SBR leads to the formation of reactive hydroxyl groups prior to the condensation reaction [39]. The silica reinforcement in SBR/D-SBR/silica composites is visualized in Scheme 1.

Mechanical properties

The stress-strain behavior of SBR/D-SBR/Silica composites containing varying proportion of D-SBR is presented in Fig. 2a. Corresponding values such as modulus at 100%, 200%, 300% elongation, tensile strength, elongation at break, tear strength and hardness are summarized in Table 2. It is seen that moduli at 100, 200 and 300% elongation steadily increase

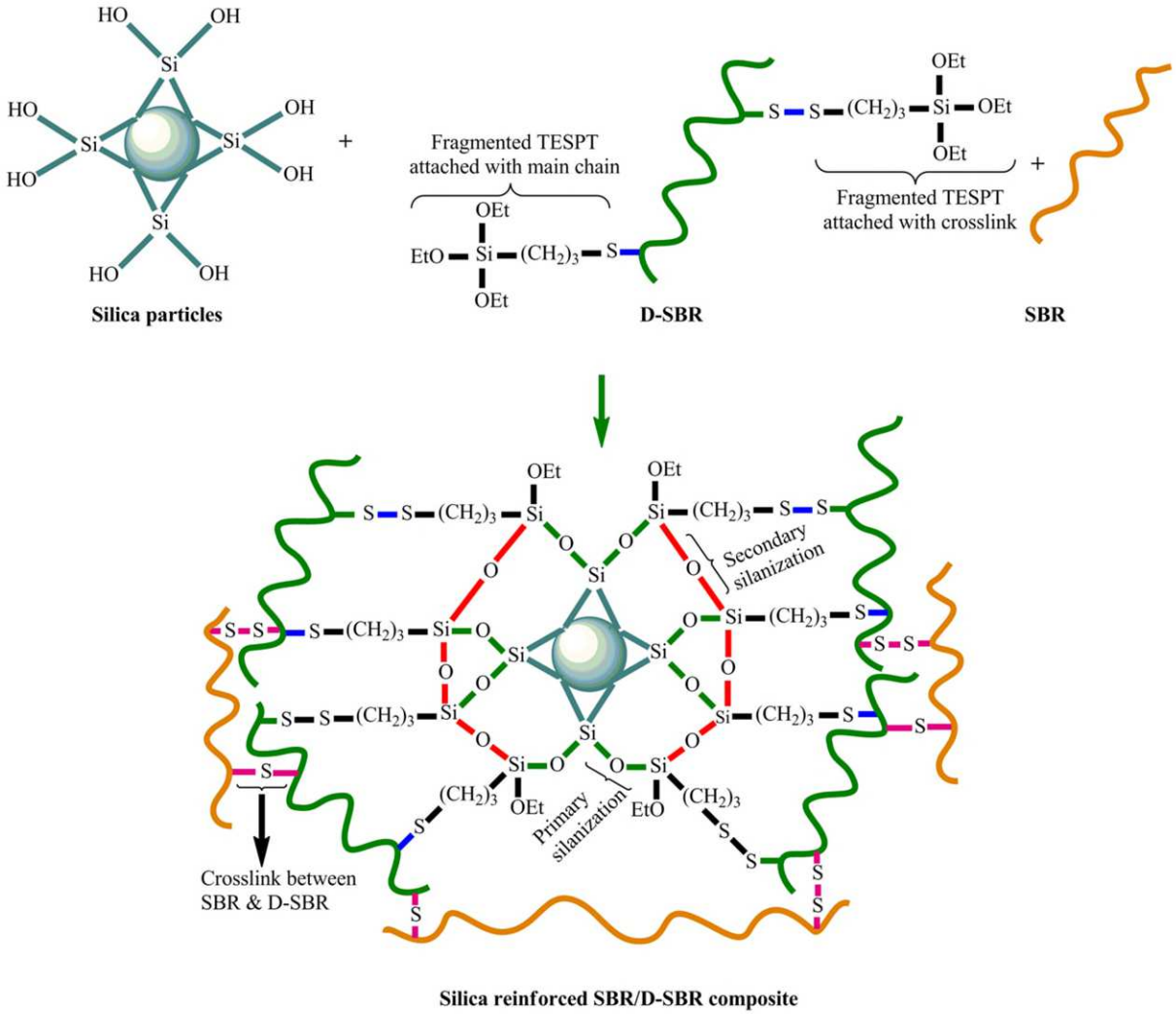

Scheme 1. Schematic presentation of silica reinforcement in SBR/D-SBR/silica composite

with D-SBR content. This behavior of the composites is associated with the increasing trend of crosslink density of the vulcanizate which is resulted from the gel present in D-SBR. This fact is also reflected from the crosslink density values of the vulcanizates presented in Fig. 2b. The

higher crosslink density value of the vulcanizates interferes the chain mobility and for this reason more load is required to stretch the rubber at a given elongation ratio. From the figures it is seen that the tensile modulus continuously increases with increasing D-SBR content and maximum tensile strength is achieved at 50 % D-SBR loading and for further increase in D-SBR content (60%) tensile modulus at given elongation decreases. The tensile strength of SBR (control) vulcanizate is much inferior to that of the SBR/D-SBR/silica vulcanizates. However, the increase in tensile strength of SBR/D-SBR/silica vulcanizates is mainly due to the strong rubber-filler interaction between pendent ethoxy group of D-SBR and the hydroxyl group present on the silica surface but for very high concentration of D-SBR content (60 %), the tensile strength slightly decreases compared to its preceding one. The inferior tensile strength value of 60 phr D-SBR loaded vulcanizate may be due to the presence of crosslinked gel present in the D-SBR which may not be homogeneously dispersed when it is mixed with fresh rubber. Such gel remains present as weak sites for stress transmission to its surrounding resulting lower tensile strength. The lower chain mobility due to increasing crosslink density of the vulcanizates decreases the elongation at break of the vulcanizates with increasing D-SBR content.

Table 2. Mechanical properties of SBR/DeVulcSBR/silica vulcanizates

Mechanical properties	**Sample Code**					
	D-0	D-20	D-30	D-40	D-50	D-60
100% Modulus (MPa)	1.59	1.94	2.58	3.48	4.33	5.17
200% Modulus (MPa)	2.60	3.36	4.48	6.52	8.71	10.34
300% Modulus (MPa)	3.82	4.97	6.91	10.01	-	-
Tensile strength (MPa)	4.28	10.26	11.03	11.53	12.26	11.9
Elongation at break (%)	336	598	475	346	278	231
Hardness (Shore A)	66.8	71	75.2	80	82	84
Tear strength (N/mm)	26.14	36.98	39.97	33.25	31.79	26.05

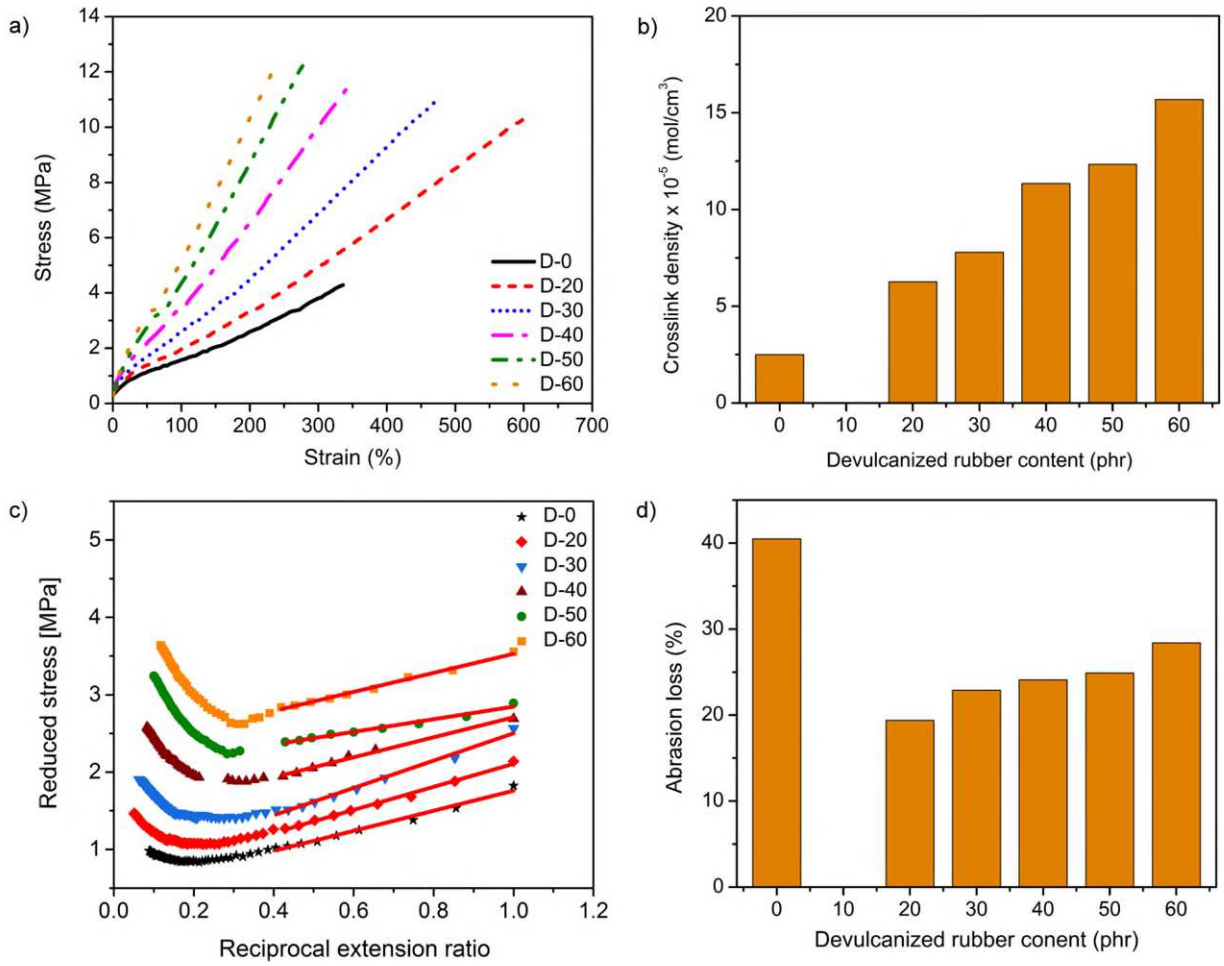

Figure 2. a) Stress-strain behavior of the rubber composites, b)effect of D-SBR content on crosslink density of SBR/D-SBR/silica vulcanizates, c) Mooney-Rivlin plot using stress-strain data, d) abrasion loss of SBR/D SBR/silica vulcanizates. In the Mooney-Rivlin figure the tangent line is drawn through the filled data pointsfrom $^{1}/_{\lambda}$ = 0.4 to 1.0.

Fig. 2c represents the Mooney-Rivlin plots of SBR/D-SBR/silica vulcanizates using equation (2). C_1 and C_2 values are obtained from the linear regime of the reduced stress ($\frac{\sigma}{\lambda-\lambda^{-2}}$) vs reciprocal extension ratio ($1/\lambda$) plot. The crosslink density from Mooney-Rivlin plot (ν_{MR}) is evaluated using equation 3. The crosslink density (ν_{MR}) are shown in Table 3. From Fig. 2c it is clearly observed that all the composites showed almost a linear region between the λ^{-1} value of 0.4 and 1.0 and it is also evident that the reduced stress (σ_r) decreases in the low λ^{-1} region due to the relaxation or slippage of the entanglements of the vulcanizates [40] and this effect is minimized

with increasing D-SBR content. However, the tendency of upturn at higher λ^{-1} region is delayed with increasing D-SBR content because D-SBR, containing short SBR chains, inhibits the symmetry of the vulcanizates as a result close packing among the rubber chains at higher λ^{-1} region due to unfolding is disturbed. In spite of delayed rise in the curve at higher λ^{-1} region, this rising becomes sharp with increasing D-SBR content. This could be attributed in terms of shorter network chain formation in the vulcanizate having higher amount of D-SBR. Moreover, another upturn in the curve up to 40 phr D-SBR loaded vulcanizates is noticed in the lower value of λ^{-1} (<0.5). This is mainly due to the non-Gaussian type of network structure. Interestingly, it is clear from the plot that the value of reduced stress increased over the entire region of λ^{-1} with higher amount of D-SBR. It indicates that a better reinforcement could be achieved due to improved elastomer-filler interaction in presence of D-SBR and the effect is more pronounced when the content of D-SBR is enhanced. The crosslink density (ν_{MR}) of the vulcanizates presented in Table 3 clearly indicates that with increasing devulcanized rubber content the crosslink density of the vulcanizates rises due to the development of higher degree of network formation among pendant ethoxy group in devulcanized rubber and silica. Moreover, the value of C_1 increases with D-SBR content is concurring with the rise of elastic torque and compound hardness due to higher crosslink density of the vulcanizates. Whereas, the value of C_2increases from 0.64 (for control vulcanizate) to 0.88 (for 30 phr D-SBR containing vulcanizate), but a scattered data is obtained for 40, 50 and 60 phr D-SBR containing vulcanizates. Furthermore, as the elastomer matrix becomes stiffer due to increasing amount of D-SBR, more and more physical entanglements are entrapped and become a part of the network.

Hardness (Table 2) also steadily increases with increasing D-SBR content. The tear strength presented in Table 2 of SBR/D-SBR/silica vulcanizates upto 40 phr D-SBR content is

much superior to that of the SBR (control) vulcanizates but for 60 phr D-SBR loading the respective values are almost comparable. The strong rubber-filler is the main reason for higher tear strength of SBR/D-SBR/silica vulcanizates up to a certain (40 phr) proportion of D-SBR. The enhanced interfacial interaction between D-SBR-silica and, consequently, the homogeneous dispersion of silica in SBR/D-SBR vulcanizate is further supported by the study of abrasion resistance of the vulcanizates.

Table 3: Summary of the Mooney-Rivlin constants and crosslink density of different SBR/D-SBR/Silica vulcanizates.

Sample name	C_1	C_2	Crosslink density $\times 10^{-4}$ (mol/cm^3)
D-0	0.23	0.64	0.92
D-20	0.30	0.74	1.21
D-30	0.37	0.88	1.49
D-40	0.70	0.65	2.82
D-50	1.01	0.40	4.07
D-60	1.15	0.61	4.64

Fig. 2d shows the abrasion loss of SBR/D-SBR/silica vulcanizates. The figure indicates that the abrasion resistance of D-SBR containing vulcanizates is much superior compared to that of the SBR (control) vulcanizates. In the control compound, the rubber to filler chemical interaction was not established due to absence of silane coupling agent in the rubber compounds which results to a rather high abrasion loss of D-0 composites. On the other hand, in devulcanized rubber containing vulcanizates, probably, stronger rubber-filler interaction by chemical coupling is the main reason for less abrasion loss of the vulcanizates.

Thermogravimetry analysis

The thermogravimetric curves (TG and DTG) of SBR (control) and different SBR/D-SBR/silica vulcanizates are presented in Fig. 3a. The degradation temperature at various weight

loss, onset and end temperature, the temperature at maximum weight loss, the rate of change of weight loss at T_{max} and char residue are shown in Table 4. The initial minor weight loss at around 145-240^{o}Cwas due to the presence of volatile matter like stearic acid and absorbed water at around 300^{o}C [41]. Although the SBR (control) vulcanizates shows one stage degradation but SBR/D-SBR/silica vulcanizates shows two stage degradation. The first stage of degradation takes place in the region of 360-425^{o}C and the second stage of degradation occurs around 425 – 515^{o}C.The first one related to the decomposition of D-SBR and the second one due to the SBR polymer decomposition [42]. There is no weight loss above 550^{o}C which indicates oxidation of carbon black present in D-SBR, originated from scrap SBR does not take place [43]. The degradation temperature at 10, 50 and 70% weight loss of SBR/DeVulcSBR/silica vulcanizates are much higher than that of the SBR (control) vulcanizates due to strong rubber-filler interaction. In SBR/D-SBR/Silica vulcanizates, the temperature at 10% weight loss and the maximum degradation temperature decrease with D-SBR content because devulcanized rubber contain large amount of processing additives. Therefore, with increasing devulcanized rubber content 10% weight loss occurs at low temperature. The temperature corresponding to 50% and 70% weight loss increases with D-SBR content due to interfacial interaction between DeVulcSBR and silica. The increase in char residue of the vulcanizates is because of the presence of increasing proportion of D-SBR in the vulcanizates. The rate of change of weight at T_{max} decreases with D-SBR content which also supports the interfacial interaction between D-SBR and silica in the SBR/D-SBR/silica vulcanizates.

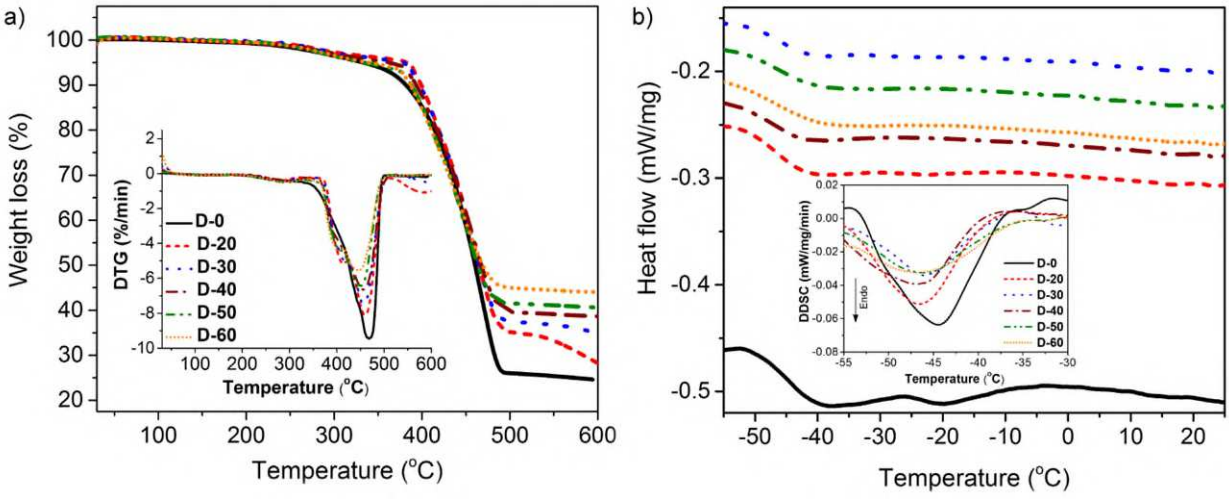

Figure 3. a) Thermogravimetry analysis; Inset: the rate of weight loss with respect to temperature b) DSC thermograms of SBR/D-SBR/silica vulcanizates

Table 4. Decomposition temperature at various weight losses of SBR/D-SBR/silica composites

Sample Code	Degradation temperature (°C)			Onset temperature (°C)	End temperature (°C)	T_{max} (°C)	The rate of change of weight at T_{max} (%/min)	% Residue
	$T_{-10\%}$	$T_{-50\%}$	$T_{-70\%}$					
D-0	381.5	460.3	482.5	344.5	500.4	469.3	9.44	24.6
D-20	399.2	464.7	583.4	368.9	508.7	460.5	8.13	23.8
D-30	397.3	464.7	669.3	365.7	512.9	456.9	7.49	27.4
D-40	393.4	467.4	-	353.7	513.7	456.9	6.64	37.8
D-50	387.3	463.2	-	359.6	506.2	447.3	6.49	39.8
D-60	386.9	469.1	-	364.6	505.1	446.0	5.55	43.2

Differential scanning calorimetry analysis

The DSC thermograms of different SBR/D-SBR/silica composites are shown in Fig. 3b and the respective values of glass transition, heat capacity increment, transition width and fraction of immobilized polymer chains are presented in Table 5. The devulcanized rubber content does not significantly affect the calorimetric glass transition temperature (T_g) but the heat capacity increment ΔC_p in the glass transition region decreases with increasing D-SBR content whichindicates that the addition of the D-SBR limited the movement of the rubber molecular chains as the surface of the silica filler produced a restricted molecular layer due to

interfacial interaction between D-SBR and silica [44]. The heat capacity increment in the glass transition region of neat rubber was maximum as SBR molecular chains were not affected by silica fillers and could move freely with high degree of freedom and as a result showing highest enthalpy. By considering ΔC_p as a measure of the quantity of devulcanized rubber that takes part in the glass transition, this decrease of $\Delta C_p$is usually considered in terms of an immobilized layer of devulcanized rubber around the silica particles. The fraction of immobilized rubber (χ_{im}) can then be evaluated by the following equations [45]:

$$\Delta C_{pn} = \frac{\Delta C_p}{(1-w)} \tag{4}$$

$$\chi_{im} = \frac{\left(\Delta C_p^0 - \Delta C_{pn}\right)}{\Delta C_p^0} \tag{5}$$

where, ΔC_p , ΔC_p^0 and w are the heat capacity increment of different D-SBR containing vulcanizates in the glass transition region, heat capacity increment of the neat rubber in the glass transition region and the weight fraction of silica respectively. Here in all the vulcanizates, silica content is fixed and only varied proportions of D-SBR are used. The fraction of immobilized polymer chains (χ_{im}) shown in Table 5 clearly specifies the effect of the D-SBR content on the freedom of motion of the rubber molecular chains. The results indicated that χ_{im} of D-60 was maximum which illustrated that D-60 had the most restricted molecular chains indicating a strong interaction between the D-SBR and silica filler [46]. This may be due to the presence of pendant ethoxy $(-OEt)$ group in the D-SBR which made the interaction between the D-SBR and the silanol $(-OH)$ groups on the silica surface [11] stronger and hence the interface bonding was improved.

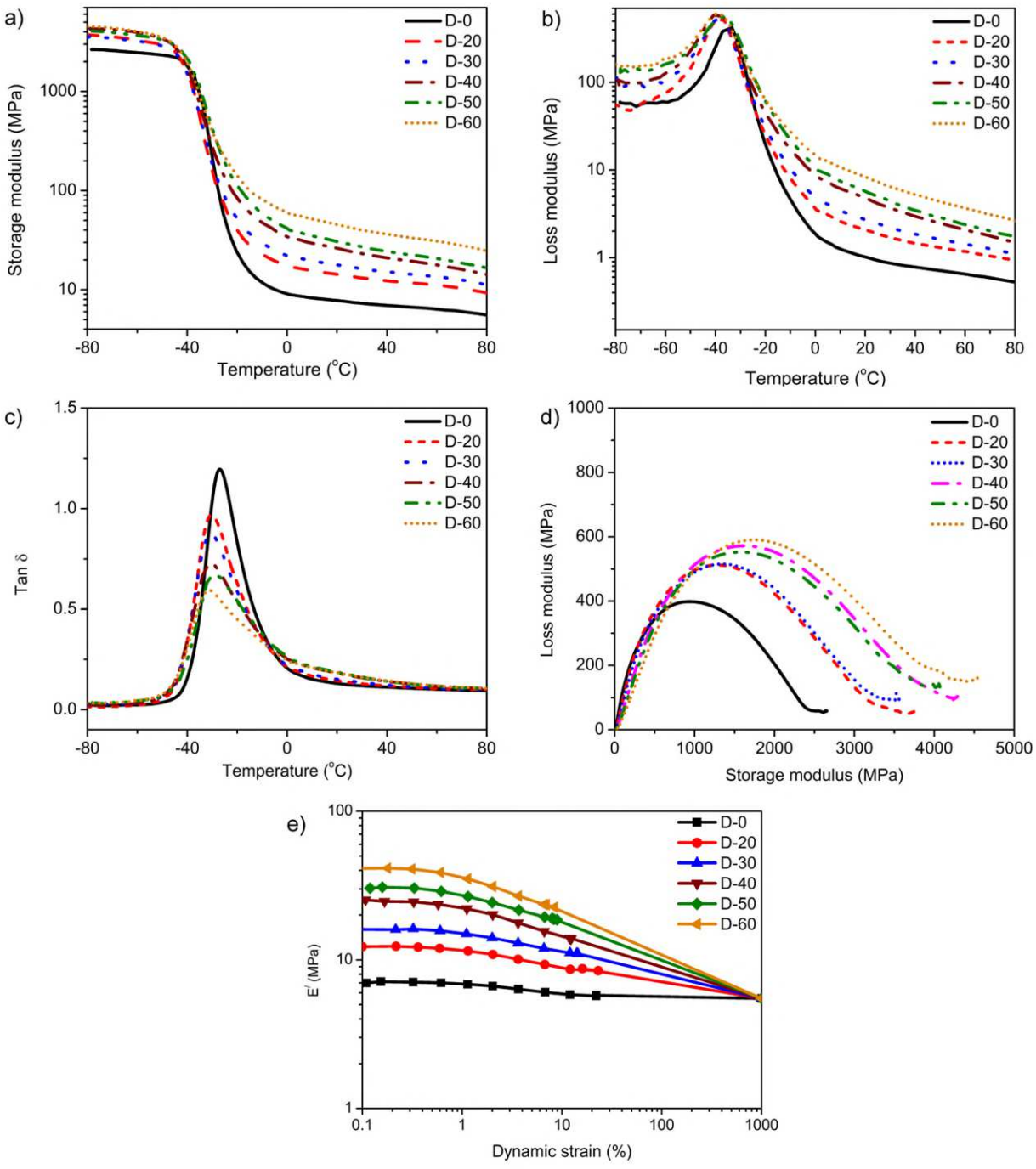

Figure 4. The dynamic mechanical analysis of the rubber composites a) storage modulus, (b) loss modulus, c) tan δ, d) Cole-Cole like plot and e) dynamic strain sweep analysis. The storage modulus at very high dynamic strain (1000 %) was calculated using Bachelor-Green equation and it is not the experimental value.

Table 5. Parameters determined from DSC measurements: glass transition temperature, heat capacity change, transition width and fraction of immobilized polymer chains of SBR/D-SBR/silica vulcanizates

Sample Code	T_g (K)	ΔC_p (J/g*K)	Δt (K)	χ_{im}
Neat rubber	232.6	0.493	12.7	-
D-0	228.7	0.207	3.6	0.466
D-20	225.7	0.142	6.3	0.633
D-30	226.5	0.077	8.8	0.801
D-40	226.8	0.061	7.2	0.844
D-50	231.3	0.058	6.2	0.850
D-60	226.2	0.019	6.3	0.951

Dynamic mechanical analysis

The interfacial interaction between rubber-filler and filler-filler greatly affects the dynamic viscoelastic properties of the vulcanizates. Generally, there are two types of networks in filler filled rubber vulcanizates, such as filler-filler network and rubber-filler network can be formed. The storage modulus, loss modulus and $\tan\delta$ of the vulcanizates are presented in Fig. 4a, 4b and 4c respectively. The storage modulus at 25 ^{o}C of SBR/D-SBR/silica vulcanizates increases with D-SBR content and the highest value is obtained for 60% D-SBR containing vulcanizates as evident from Fig. 4a and Table 6. However, the room temperature storage modulus of SBR (control) vulcanizates is much inferior than that of the D-SBR containing vulcanizates due to strong filler-filler interaction as a result silica agglomerates are formed in the rubber matrix which is responsible for poor compatibility of silica filler in the fresh SBR, whereas, in D-SBR containing vulcanizates the respective values are much higher due to interfacial interaction between the ethoxy group of D-SBR and hydroxyl group of silica.

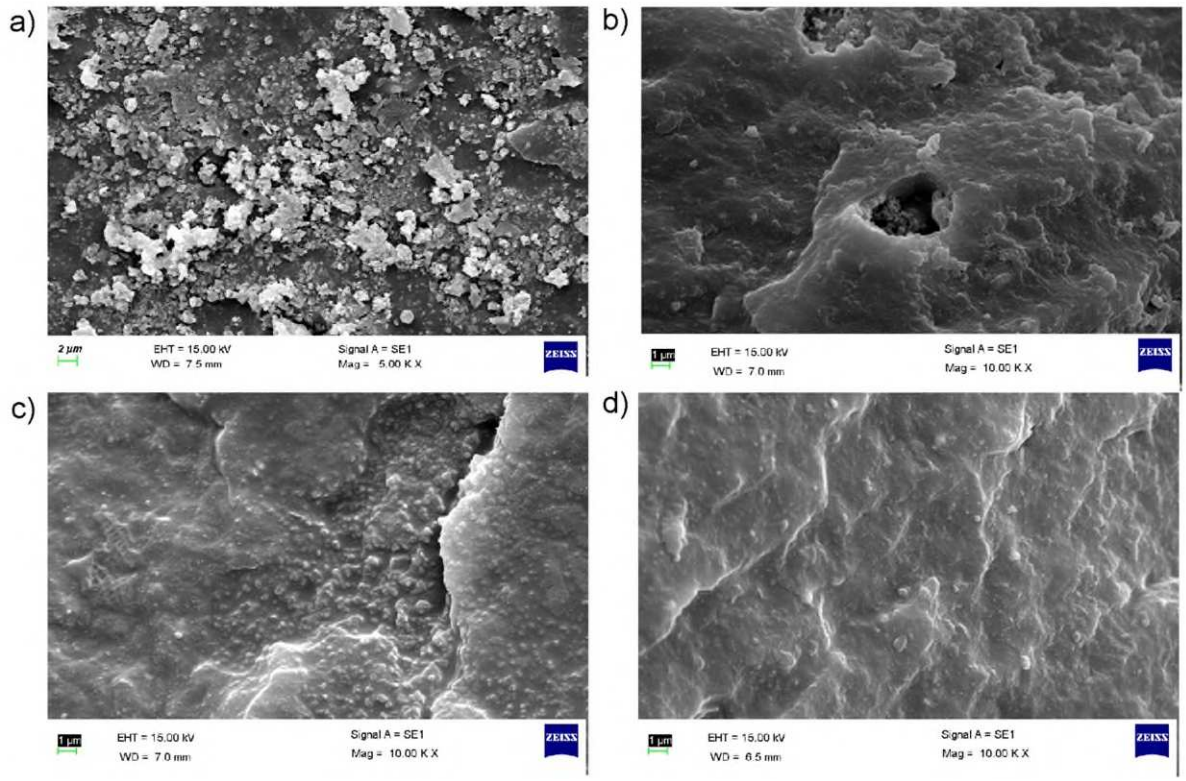

Figure 5. SEM micrograph of (a) D-0; (b) D-20; (c) D-40 and (d) D-50.

The temperature dependence of loss modulus of SBR (control) and different SBR/D-SBR/silica vulcanizates is presented in Fig. 4b. From the figure it is evident that loss modulus of D-SBR containing vulcanizates increases with D-SBR content. The behavior of loss modules is expected to show the same trend like storage modulus, shown in the figure.

The temperature dependence of $\tan\delta$ of SBR (control) and SBR/D-SBR/silica vulcanizates is shown in Fig. 4c. From this figure it is evident that the position of loss tangent $(tan\,\delta_{\max})$ is slightly shifted towards low temperature with increasing amount of D-SBR. All the vulcanizates show the glass transition in the narrow temperature range from -27.2 ^{o}C to -31.2 ^{o}C. From Table 6 it is seen that $tan\,\delta_{max}$ is consistently decreased with increased D-SBR content indicating more non-elastic component in the rubber matrix. More bound rubber and higher reinforced state of the rubber matrix could be the reason behind such behavior.

The impact of filler reinforcement can also be explained in terms of Cole-Cole type plots. Here, the moduli plots E'' vs. E' from the temperature sweeps of SBR/D-SBR/silica vulcanizates are presented in Fig. 4d. From the figure it is evident that irrespective of devulcanized rubber concentration all the D-SBR vulcanizates show depressed semicircle, which indicates the presence of reinforcing filler in the vulcanizate. The higher D-SBR containing vulcanizate shows large arc than that of the lower D-SBR containing vulcanizates because higher D-SBR containing vulcanizate exhibits greater rubber-filler interaction due to the presence of large number of ethoxy ($-OEt$) groups. All the curves show smooth arcs indicating homogeneous dispersion of silica in the rubber matrix.

Table 6. Values of G/, $Tan\ \delta_{max}$ and T_g of SBR/D-SBR composite

Sample Code	$G^{/}$ (MPa) at 25°C	$Tan\ \delta_{max}$	T_g at peak temperature (°C)
D-0	7.62	1.20	-27.0
D-20	13.68	0.97	-29.9
D-30	16.90	0.88	-30.6
D-40	24.31	0.73	-31.2
D-50	28.66	0.69	-29.1
D-60	42.73	0.60	-31.2

The strain sweep analysis at room temperature is shown in Fig. 4e. It can be found that, as expected, the D-0 shows a little dependency of the storage modulus on the dynamic strain amplitude, however, the modulus further increases with increasing D-SBR loadings. This substantiates the formation of both reinforcing networks: filler-filler and filler-polymer networks which the last one is defined as the Payne effect [47]. The overall dynamic performance here is mainly governed by different factors like the chemical activity of the active groups of the devulcanized rubber, the presence of sulphur curatives in the recycled rubber, pre-crosslinked

rubber molecules, fragments of the devulcanized rubber chains and the final results are the complex interplays between all those factors. More studies are further needed to understand the overall mechanical properties of the devulcanized rubber composites.

SEM analysis

Fig.5 corresponds to the SEM images of the tensile fractured surface of SBR/silica (Fig. 5a) and representative figures of different SBR/D-SBR/silica composites containing D-SBR 20 phr (Fig. 5b), 40 phr (Fig. 5c) and 50 phr (Fig. 5d). It is evident from Fig. 5a that silica is unevenly dispersed in SBR matrix due to the presence of large silica agglomerates for the formation of hydrogen bonds among the abundant silanol groups on its surface [48]. However, in D-SBR containing vulcanizates most of the silanol groups react with the ethoxy functionality of D-SBR and as a result the agglomerates of silica particles get reduced. This chemical reaction changes the hydrophilic silica particles to hydrophobic in nature [49] which ultimately make silica particles compatible in SBR/D-SBR matrix through the formation of a coating of a thin layer of rubber on the silica surface as evident from Fig. 5b, 5c & 5d. Moreover, it is evident from Fig. 5b, c & d that with increasing D-SBR content the silica surfaces are well covered by a skinny layer of rubber. It is also seen from the D-SBR containing micrographs that in higher D-SBR loaded composites (Fig. 5c & 5d) the maximum matrix tearing line and surface roughness is observed compared to that of the Fig. 5b having lower D-SBR content. A superior rubber-filler interaction in Fig. 5c & 5d altered the fracture path, which led to increased resistance to fracture propagation that resulted an increase in tensile modulus, tensile strength and hardness of the composites as evident from the performance of the mechanical properties of the composites. The micrographs of the tensile fractured surfaces were in good concurrence with the results studied

by other researchers [50, 51] who stated that surface roughness and matrix tearing lines in the fractured surface occurred due to increase in rupture energy.

Conclusion

The research describes a unique technology to devulcanize waste rubber and its subsequent application in silica reinforced SBR/D-SBR vulcanizates. The conclusions based on the silica reinforcement in SBR/D-SBR composites by FTIR study, SEM micrographs analysis, mechanical and dynamic mechanical properties and thermal behavior are summarized as follows:

- FTIR study of the composites reveals the chemical bond formation between the pendant ethoxy ($-OEt$) group in D-SBR and the hydroxyl ($-OH$) group on the silica surface by appearance of $Si-O-Si$ stretching at 1105 cm^{-1} and disappearance of $-OH$ stretching at 3446 cm^{-1}.
- The mechanical properties of the composites clearly specify that the tensile strength and tear strength of the composites increase up to 50 phr and 30 phr D-SBR content respectively. The tensile strength of 50 phr D-SBR containing composite is 286% higher and tear strength of 30 phr D-SBR bearing composite is 152% higher than that of the control SBR vulcanizates.
- The thermogravimetric analysis of the composites signifies the improvement of thermal stability in presence of D-SBR in compared to that of the control SBR vulcanizates.
- The DSC analysis further confirms the rubber – filler interaction by decrease of the heat capacity increment (ΔC_p) in the glass transition region as well as the increase of fraction of immobilized polymer chains (χ_{im}) with increasing D-SBR content.

- Dynamic mechanical properties of the composite indicate that the addition of D-SBR has no significant effect on the T_g but on increasing D-SBR loading, the $tan\ \delta_{max}$ decreases. Moreover, the complete semicircular Cole-Cole type plot authenticates the nonlinear/non – Debye type of relaxation of the composites and the smoothness of the curves irrespective of the D-SBR loadings indicates good dispersion of D-SBR in the composite.
- SEM micrographs indicate the homogeneous surface morphology of the composites in which silica surfaces are covered by thin layer of rubber.

Acknowledgement

The authors thankfully acknowledge the financial support by the Department of Science and Technology (DST), Science and Engineering Research Board (SERB), New Delhi, India, (Project No. SB/S3/ME/40/2013 Dated April 09, 2014) for carrying out the present research work.

References

[1] Sekhar, G.B. Proceedings of the tire technology expo, Cologne, Germany, 2014.

[2] Adhikari, B., De, D., Maiti, S.: Reclamation and recycling of waste rubber. Prog. Polym. Sci. 25, 909-948 (2000). https://doi.org/10.1016/S0079-6700(00)00020-4

[3] Seghar, S., Asaro, L., Rolland-Monnet, M., Hocine, N.A.: Thermomechanical devulcanization and recycling of rubber industry waste. Resour. Conserv. Recyl. 144, 180-186 (2019). https://doi.org/10.1016/j.resconrec.2019.01.047

[4] Si, H., Chen, T., Zhang, Y.: Effects of high shear stress on the devulcanization of ground tire rubber in a twin-screw extruder. J. Appl. Polym. Sci. 128, 2307-2318 (2013). https://doi.org/10.1002/app.38170

[5] Prut, E., Solomatin, D., Kuznetsova, O., Tkachenko, L., Khalilov, D.: Grinding of ethylene-propylene-diene monomer vulcanizates. High-temperature sintering of rubber powder. J. Elast. Plast. 47, 52-68 (2013). https://doi.org/10.1177%2F0095244313489905

[6] Yazdani, H., Karrabi, M., Ghasmi, I., Azizi, H., Bakhshandeh, G.R.: Devulcanization of waste tires using a twin-screw extruder: The effects of processing conditions. J. Vinyl Additv. Technol. 17, 64-69 (2011). https://doi.org/10.1002/vnl. 20257

[7] De, D., Das, A., De, D., Dey, B., Debnath, S.C., Roy, B.C.: Reclaiming of ground rubber tire (GRT) by a novel reclaiming agent. Europ. Polym. J. 42, 917-927 (2006). https://doi.org/10.1016/ j.eurpolymj.2005.10.003

[8] Ghorai, S., Bhunia, S., Roy, M., De, D.: Mechanochemical devulcanization of natural rubber vulcanizate by dual function disulfide chemicals. Polym. Degrad. Stab. 129, 34-46 (2016). https://doi.org/10.1016/j.polymdegradstab.2016.03.024

[9] Ghosh, J., Ghorai, S., Bhunia, S., Roy, M., De, D.: The role of devulcanizing agent for mechanochemical devulcanization of styrene butadiene rubber vulcanizate. Polym. Eng. Sci. 58, 74-85 (2018). https://doi.org/10.1002/pen.24533

[10] Ghorai, S., Mondal, D., Hait, S., Ghosh, A.K., Weissner, S., Das, A., De, D.: Devulcanization of waste rubber and generation of active sites for silica reinforcement. ACS Omega 4, 17623-17633 (2019). https://doi.org/10.1021/acsomega.9b01424

[11] Ghosh, J., Hait, S., Ghorai, S., Mondal, D., Wiessner, S., Das, A., De, D.: Cradle-to-cradle approach to waste tyres and development of silica based green tyre composites. Resour. Conserv. Recyl. 154, 104629(1-13) (2020). https://doi.org/10.1016/j.resconrec.2019. 104629

[12] De, D., Roy, M., Das, S., Ghorai, S., Jalan, A.K.: Mechanochemical reclaiming of ground rubber tire using a dual-functional reclaiming agent. Plastic Research Online. 26 June, (2017). https://doi.org/10.2417/spepro.006911

[13] Movahed, S.O., Ansarifar, A., Zohuri, G., Ghaneie, N., Kermany, Y.: Devulcanization of ethylene–propylene–diene waste rubber by microwaves and chemical agents. J. Elast. Plast. 48, 122-144 (2014). https://doi.org/10.1177%2F009524 4314557975

[14] Zanchet, A., Carli, L.N., Giovanela, M., Crespo, S.J., Scuracchio, C.H., Nunes, C.R.R.: Characterization of Microwave- Devulcanized Composites of Ground SBR Scraps. J. Elast. Plast. 41, 497-507 (2009). https://doi.org/10.1177%2F0095244309345411

[15] Luo, M., Liao, X., Liao, S., Zhao, Y.: Mechanical and dynamic mechanical properties of natural rubber blended with waste rubber powder modified by both microwave and sol–gel method. J. Appl. Polym. Sci. 129, 2313-2320 (2013). https://doi.org/10.1002/app.38954

[16] Ghose, S., Isayev, A.I.: Ultrasonic Devulcanization of Carbon Black Filled Polyurethane Rubber. J. Elast. Plast. 36, 213-239 (2004). https://doi.org/10.1177%2F 0095244304042598

[17] Hong, C.K., Isayev, A.I.: (2001) Plastic/rubber blends of ultrasonically devulcanized GRT with HDPE. J. Elast. Plast. 33, 47-71 (2001). https://doi.org/10.1106%2F5AMQ-XEAY-A05B-P1FY.

[18] Bockstal, L., Berchem, T., Schmetz, Q., Richel, A.: Devulcanization and reclaiming of tires and rubber by physical and chemical processes: A review. J. Clean. Prod. 236, 117574 (1-16) (2019). https://doi.org/10.1016/j.jclepro.2019.07.049

[19] Sienkiewicz, M., Janik, H., Borzedowska-Labuda, K., Kucinska-Lipka, J.: Environmentally friendly polymer-rubber composites obtained from waste tyres: A review. J. Clean. Prod. 14, :560-571 (2017). https://doi.org/10.1016/j.jclepro.2017.01.121

[20] Zedler, Ł., Przybysz, M., Klein, M., Saeb, M.R., Formela, K.: (2017) Processing, physico-mechanical and thermal properties of reclaimed GTR and NBR/reclaimed GTR blends as function of various additives. Polym. Degrad. Stab. 143, 186-195 (2017). https://doi.org/10.1016/j. polymdegradstab.2017.07.004

[21] Sabzekar, M., Zohuri, G., Chenar, M.P., Mortazavi, S.M., Kariminejad, M., Asadi, S.: (2016) A new approach for reclaiming of waste automotive EPDM rubber using waste oil. Polym. Degrad. Stab. 129, 56-62 (2016). https://doi.org/10.1016/j.polymdegradstab.2016.04.002

[22] De, D., Panda, P.K., Roy, M., Bhunia, S.: Reinforcing effect of reclaim rubber on natural rubber/polybutadiene rubber blends. Mat. Des. 46, 142-150 (2013). https://doi.org/10.1016/j.matdes. 2012.10.014

[23] Morsi, S.M.M., Mohamed, H.A., El-Sabbagh, S.H.: Polyesteramidesulfone as novel reinforcement and antioxidant nanofiller for NBR blended with reclaimed natural rubber. Mat. Chem. Phys. 224, 206-216 (2019). https://doi.org/10.1016/j.matchemphys.2018.12.017

[24] Karabork, F., Pehlivan, E., Akdemir, A.: Characterization of styrene butadiene rubber and microwave devulcanized waste tire rubber composites. J. Polym. Engg. 34, 543-554 (2014). https://doi.org/10.1515/polyeng-2013-0330

[25] Hassan, M.M., Badway, N.A., Elnaggar, M.Y., Hegazy, E.A.: Effects of peroxide and gamma radiation on properties of devulcanized rubber/polypropylene/ethylene

propylene diene monomer formulation. J. Appl. Polym. Sci. 131, 40611(1-10) (2014). https://doi.org /10.1002/app.40611

[26] Formela, K., Cysewska, M., Haponiuk, J.T.: (2016) Thermomechanical reclaiming of ground tire rubber via extrusion at low temperature: Efficiency and limits. J. Vinyl Addit. Technol. 22, 213-221 (2016). https://doi.org/10.1002/vnl.21426

[27] Dobrota, D., Dobrota, G.: An innovative method in the regeneration of waste rubber and the sustainable development. J. Clean. Prod. 172, 3591-3599 (2018). http://dx.doi.org /10.1016/j.jclepro. 2017.03.022

[28] Phiri, M.M., Sibeko, M.A., Phiri, M.J., Hlangothi, S.P.: Effect of the free foaming and pre-curing on the thermal, morphological and physical properties of reclaimed tyre rubber foam composites. J. Clean. Prod. 218, 665-672 (2019). https://doi.org/10.1016/j.jclepro.2019.02.051

[29] Liu, H.L., Wang, X.P., Jia, D.M.: Recycling of waste rubber powder by mechano-chemical modification. J. Clean. Prod. 245, 118716 (2020). https://doi.org/10.1016/j.jclepro.2019.118716

[30] Tseng, H.H., Lin, Z.Y., Chen, S.H., Lai, W.H., Wey, M.Y.: Reuse of reclaimed tire rubber for gas-separation membranes prepared by hot pressing. J Clean Prod 237, 117739(1-11) (2019). https://doi.org/10.1016/j.jclepro.2019.117739

[31] Zhang, X., Sinha, T.K., Ahn, Y., Kim, J.K.: Temperature dependent amphoteric behavior of bis[3-(triethoxysilyl) propyl] tetrasulfide towards recycling of waste rubber: A triboelectric investigation. J. Clean. Prod. 213, 569-576 (2019). https://doi.org/10.1016/j.jclepro.2018.12.149

[32] De, D., Maiti, S., Adhikari, B.: Reclaiming of rubber by a renewable resource material (RRM). III. Evaluation of properties of NR reclaim. J. Appl. Polym. Sci. 75, 1493-1502 (2000). https://doi.org/10.1002/(SICI)1097-4628(20000321)75:12%3C1493::AID-APP8%3E3.0.CO;2-U

[33] Mooney, M.: A theory of large elastic deformation. J Appl Phys 11, 582-592 (1940). https://doi. org/10.1063/1.1712836

[34] Rivlin, R.S., Saunders, D.W.: Large elastic deformations of isotropic materials VII. Experiments on the deformation of rubber. Philosophical Trans Royal Soc A 243:251-288 (1951). https://doi.org/10.1098/rsta.1951.0004

[35] Eisele, U.: Introduction to Polymer Physics, Springer-Verlag, Berlin Heidelberg. (1990) http://doi -org-443.webvpn.fjmu.edu.cn/10.1007/978-3-642-74434-1_7.

[36] Graessley, W.W.: The entanglement concept in polymer rheology. In: The entanglement concept in polymer rheology, Advances in Polymer Science, Springer, Berlin, Heidelberg, Vol 16, pp 1-79 (1974).

[37] Andrew, C.: An introduction to rubber technology, 1st Edition, Rapra Technology Ltd., Germany (1999).

[38] Alan, N.G.: Engineering with rubber – How to design rubber components, 2nd Edition, Hanser Publishers, Munich (2001).

[39] Görl, U., Hunsche, A., Mueller, A., Koban, H.G.: Investigations into the silica/silane reaction system. Rubber Chem Technol 70, 608–623 (1997). https://doi.org/10.5254/1.3538447

[40] Huang, C., Huang, G., Li, B., Luo, M., Liu, H., Fu, X., Qu, W., Xie, Z., Wu, J.: Research on architecture and composition of natural network in natural rubber. Polymer 154, 90-100 (2018). https://doi.org/10.1016/j.polymer.2018.08.057

[41] Tomer, N., Delor-Jestin, F., Singh, R., Lacste, J.: Cross-linking assessment after accelerated aging of ethylene propylene diner monomer rubber. Polym. Degrad. Stab. 92, 457-463 (2007). https://doi.org/10.1016/j.polymdegradstab.2006.11.013

[42] Williams, P.T., Bessler, S.: Pyrolysis-thermogravimetric analysis of tyres and tyre components. Fuel 74, 1277-1283 (1995). https://doi.org/10.1016/0016-2361(95)00083-H

[43] Karabork, F., Akdemir, A.: Friction and wear behavior of styrene butadiene rubber-based composites reinforced with microwave-devulcanized ground tire rubber. J. Appl. Polym. Sci. 132:42419 (1-9) (2015). https://doi.org/10.1002/app.42419

[44] Karger-Kocsis, J., Wu, C.M.: Thermoset rubber/layered silicate nanocomposites. Status and future trends. Polym. Eng. Sci. 44(6), 1083–1093 (2004). https://doi.org/10.1002/pen.20101

[45] Li, Y., Ishida, H.: A Study of Morphology and Intercalation Kinetics of Polystyrene−Organoclay Nanocomposites. Macromolecules 38(15), 6513-6519 (2005). https://doi.org/ 10.1021/ma0507084

[46] Zhong, B., Jia, Z., Hu, D., Luo, Y., Guo, B., Jia, D.: Surface modification of halloysite nanotubes by vulcanization accelerator and properties of styrene-butadiene rubber nanocomposites with modified halloysite nanotubes. Appl. Surf. Sci. 366, 193-201 (2016). https://doi. org/10.1016/j.apsusc.2016.01.084

[47] Haghtalab, A., Marzbank, R.: Viscoelastic properties of nanosilica-filled polypropylene in the molten state: effect of particle size. Adv Polym Technol 30, 203-218 (2011). https://doi.org/ 10.1002/adv.20217

[48] Liu, X., Zhao, S., Zhang, X., Li, X., Bai, Y.: Preparation, structure and properties of solution-polymerized styrene butadiene rubber with functionalized end groups and its silica filled composites. Polymer 55(8), 1964-1976 (2014). https://doi.org/10.1016/j.polymer.2014.02.067

[49] Fröhlich, J., Niedermeier, W., Luginsland, H.D.: The effect of filler-filler and filler-elastomer interaction on rubber reinforcement. Compos. Part A: Appl. Sci. Manuf. 36(4), 449-460 (2005). https://doi.org/10.1016/j.compositesa.2004.10.004

[50] Ismail, H., Mathialagan, M.: Comparative study on the effect of partial replacement of silica or calcium carbonate by bentonite on the properties of EPDM composites, Polym. Test. 31, 199-208 (2012). https://doi.org/10.1016/j.polymertesting.2011.09.002

[51] Nabil, H., Ismail, H., Azura, A.: Compounding, mechanical and morphological properties of carbon-black-filled natural rubber/recycled ethylene-propylene-diene-monomer (NR/R-EPDM) blends, Polym Test 32, 385-393 (2013). https://doi.org/10.1016/j.polymertesting.2012.11.003

Figure for Table of Content